Oncogene (2005) 24, 7592–7598

www.nature.com/onc

MEK kinase 1 is essential for Bcr–Abl-induced STAT3 and self-renewal activity in embryonic stem cells

Yukinori Nakamura[1], Toshiaki Yujiri*,[1], Ryouhei Nawata[1], Kozo Tagami[1] and Yukio Tanizawa[1]

[1]*Department of Bio-Signal Analysis, Yamaguchi University Graduate School of Medicine, 1-1-1 Minami Kogushi, Ube, Yamaguchi 755-8505, Japan*

BCR–ABL oncogene, the molecular hallmark of chronic myelogenous leukemia, arises in a primitive hematopoietic stem cell that has the capacity for both differentiation and self-renewal. Its product, Bcr–Abl protein, has been shown to activate signal transducers and activators of transcription 3 (STAT3) and to promote self-renewal in embryonic stem (ES) cells, even in the absence of leukemia inhibitory factor (LIF). MEK kinase 1 (MEKK1) is a 196-kDa mitogen-activated protein kinase (MAPK) kinase kinase involved in Bcr–Abl signal transduction. To investigate the role of MEKK1 in Bcr–Abl-induced transformation of stem cells, p210 Bcr–Abl was stably transfected into wild-type (WT^{p210}) and MEKK1−/− ($MEKK1-/-^{p210}$) ES cells. Bcr–Abl enhanced MEKK1 expression in ES transfectants, as it does in other Bcr–Abl-transformed cells. In the absence of LIF, WT^{p210} cells showed constitutive STAT3 activation and formed rounded, compact colonies having strong alkaline phosphatase activity, a characteristic phenotype of undifferentiated ES cells. $MEKK1-/-^{p210}$ cells, by contrast, showed less STAT3 activity than WT^{p210} cells and formed large, flattened colonies having weak alkaline phosphatase activity, a phenotype of differentiated ES cells. These results indicate that MEKK1 plays a key role in Bcr–Abl-induced STAT3 activation and in ES cells' capacity for LIF-independent self-renewal, and may thus be involved in Bcr–Abl-mediated leukemogenesis in stem cells.
Oncogene (2005) **24,** 7592–7598. doi:10.1038/sj.onc.1208899; published online 25 July 2005

Keywords: Bcr–Abl; MEKK1; STAT3; embryonic stem cell

Introduction

Chronic myelogenous leukemia (CML) is a neoplasm arising from primitive hematopoietic cells expressing the 210-kDa form of Bcr–Abl, a chimeric oncoprotein generated by the reciprocal translocation t(9;22) (Deininger *et al*., 2000). This oncoprotein is responsible for the phosphorylation, activation and dysregulation of various intracellular signaling proteins that regulate the proliferation and survival of progenitor cells. Patients with CML have a rare but consistently detectable population of quiescent Bcr–Abl-positive $CD34^+$ cells (Holyoake *et al*., 1999) that possess an ability for self-renewal and contribute to the disease's pathogenesis. One recent study showed that Bcr–Abl constitutively activates signal transducers and activators of transcription 3 (STAT3) and promotes self-renewal of embryonic stem (ES) cells, even in the absence of leukemia inhibitory factor (LIF). Similarly, $CD34^+$ cells purified from CML patients show increased levels of STAT3 activation (Coppo *et al*., 2003).

MEK kinase 1 (MEKK1) is a 196-kDa mitogen-activated protein kinase (MAPK) kinase kinase that is activated in response to a variety of stimuli, and has been shown to participate in the regulation of c-Jun N-terminal kinase (JNK) and extracellular signal regulated kinase (ERK) activity, and to be involved in the activation of NF-κB (Hagemann and Blank, 2001). In addition, we previously showed that cell transformation induced by Bcr–Abl leads to increased expression of MEKK1, which then serves as a downstream target of Bcr–Abl, mediating an antiapoptotic effect (Nawata *et al*., 2003). To investigate the role of MEKK1 in Bcr–Abl-induced transformation of stem cells, we used a stable line of p210 Bcr–Abl-transfected MEKK1−/− ES cells to examine the effects of disrupting MEKK1 expression on the Bcr–Abl-induced undifferentiated phenotype and constitutive STAT3 activation. Our findings show for the first time that the MEKK1–STAT3 pathway is a downstream target of Bcr–Abl that mediates maintenance of the undifferentiated phenotype of ES cells.

Results

Bcr–Abl increases MEKK1 expression in ES cells

We began investigating the relationship between Bcr–Abl and MEKK1 by evaluating MEKK1 expression in p210 Bcr–Abl-transformed ES cells. We found that expression of MEKK1 protein was constitutively increased in Bcr–Abl-transformed wild-type (WT^{p210}) cells, as compared to green fluorescent protein (GFP)-trans-

*Correspondence: T Yujiri;
E-mail: yujirit@yamaguchi-u.ac.jp
Received 9 February 2005; revised 3 June 2005; accepted 3 June 2005; published online 25 July 2005

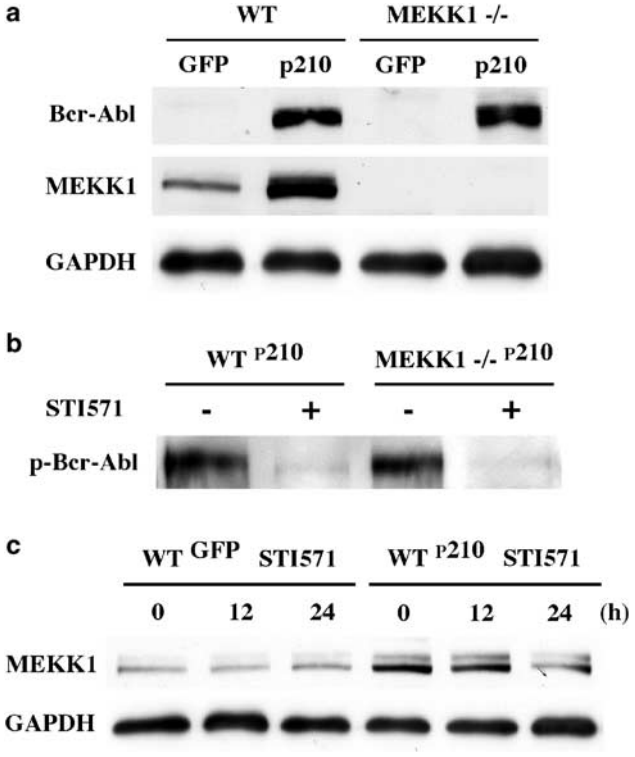

Figure 1 Bcr–Abl enhances expression of MEKK1 in ES cells. (**a**) ES cells were harvested and lysed, after which the cell lysates were immunoblotted for Bcr–Abl and MEKK1. (**b**) Bcr–Abl-transformed WT and MEKK1−/− ES cells were treated with 10 μM STI571 for 24 h. The cell lysates were then immunoprecipitated for Bcr–Abl using anti-c-Abl Ab and immunoblotted with 4G10. (**c**) GFP- or Bcr–Abl-transformed WT ES cells were treated with 10 μM STI571 for the indicated times, after which the cell lysates were immunoblotted for MEKK1. Levels of GAPDH confirmed that equivalent amounts of protein had been loaded into each lane (**a**, **c**). The immunoblotting shown is representative of three independent experiments yielding similar results

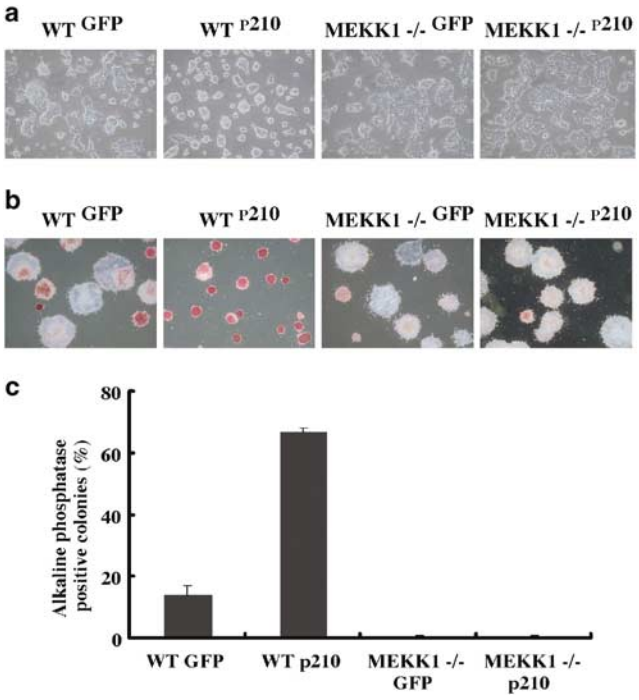

Figure 2 MEKK1 is required for Bcr–Abl-induced inhibition of ES cell differentiation in the absence of LIF. (**a**) ES cells were seeded onto uncoated culture dishes in the absence of LIF, and 48 h later their morphology was evaluated. (**b**) ES cells were seeded onto uncoated culture dishes in the presence of LIF and cultured for 3 days, after which the LIF was removed from the medium for 2 days and alkaline phosphatase activity was assayed. (**c**) ES cells were scored for alkaline phosphatase activity by microscopic examination. The percentage of colonies that were alkaline phosphatase-positive was calculated by scoring 100 randomly chosen cells. Data represent means ± s.d. of three independent experiments

formed WT (WT^{GFP}) cells. Furthermore, *in vitro* kinase assays confirmed that the level of MEKK1 activity was greater in WT^{p210} than WT^{GFP} cells (data not shown). Neither GFP- nor Bcr–Abl-transformed MEKK1−/− cells (MEKK1−/$-^{GFP}$ and MEKK1−/$-^{p210}$) expressed MEKK1 (Figure 1a).

To investigate the relationship between Bcr–Abl activity and MEKK1 expression in more detail, we next examined the effects of imatinib mesylate (STI571), a selective inhibitor of Bcr–Abl tyrosine kinase activity (Druker, 2002). In both WT^{p210} and MEKK1−/$-^{p210}$ cells, STI571 treatment reduced the level of autophosphorylated Bcr–Abl, which is indicative of reductions in Bcr–Abl tyrosine kinase activity (Figure 1b). In addition, there was a corresponding time-dependent decline in the expression of MEKK1 in WT^{p210} cells; expression of MEKK1 in WT^{GFP} cells was unaffected (Figure 1c). Taken together, these results indicate that Bcr–Abl increases MEKK1 expression in ES cells and that the effect is largely dependent on Bcr–Abl tyrosine kinase activity.

MEKK1 is required for inhibition of ES cell differentiation by Bcr–Abl

Introduction of the Bcr–Abl oncogene into WT and MEKK1−/− ES cells did not induce any growth advantage beyond the control (data not shown). On the other hand, we found that, under conventional culture conditions, colonies of growing WT^{p210} cells were morphologically rounder and more compact than colonies of nontransformed WT cells. To better understand these morphological changes, we cultured ES cells on uncoated culture dishes without LIF. Under those conditions, WT^{p210} cells formed compact, rounded colonies, a phenotype characteristic of undifferentiated ES cells. By contrast, MEKK1−/$-^{p210}$ cells showed large, flattened colonies, a phenotype characteristic of differentiated ES cells (Figure 2a). To confirm the differentiation status of cells, we measured alkaline phosphatase activity (Pease *et al*., 1990) and found that, whereas about 67% of WT^{p210} cells were alkaline phosphatase-positive in the absence of LIF, MEKK1−/$-^{p210}$ cells were almost all alkaline phosphatase-negative (Figure 2b and c). This suggests that Bcr–Abl confers the ability to maintain an undifferentiated state in the absence of LIF, and that this effect is mediated by MEKK1.

MEKK1 is essential for Bcr–Abl-induced STAT3 activation

LIF-induced STAT3 activation is essential for maintaining an undifferentiated state in ES cells (Burdon *et al*., 2002), although one recent study showed that Bcr–Abl constitutively activates STAT3, thereby promoting self-renewal in ES cells even in the absence of LIF (Coppo *et al*., 2003). We therefore investigated the extent to which MEKK1 is involved in Bcr–Abl-induced STAT3 activation. Using immunoblot analyses, we found that, in the absence of LIF, STAT3 was more strongly phosphorylated on both Tyr705 and Ser727 in WT^{p210} cells than in WT^{GFP} cells, and that the increased phosphorylation was associated with an increase in the level of total STAT3 protein. By contrast, the level of phosphorylated STAT3 in MEKK1$-/-^{p210}$ cells was similar to that in MEKK1$-/-^{GFP}$ cells (Figure 3a–d), which suggests that MEKK1 is required for Bcr–Abl-induced STAT3 expression and phosphorylation. Evaluation of Bcr–Abl-induced STAT3 mRNA expression using semiquantitative RT–PCR analysis showed

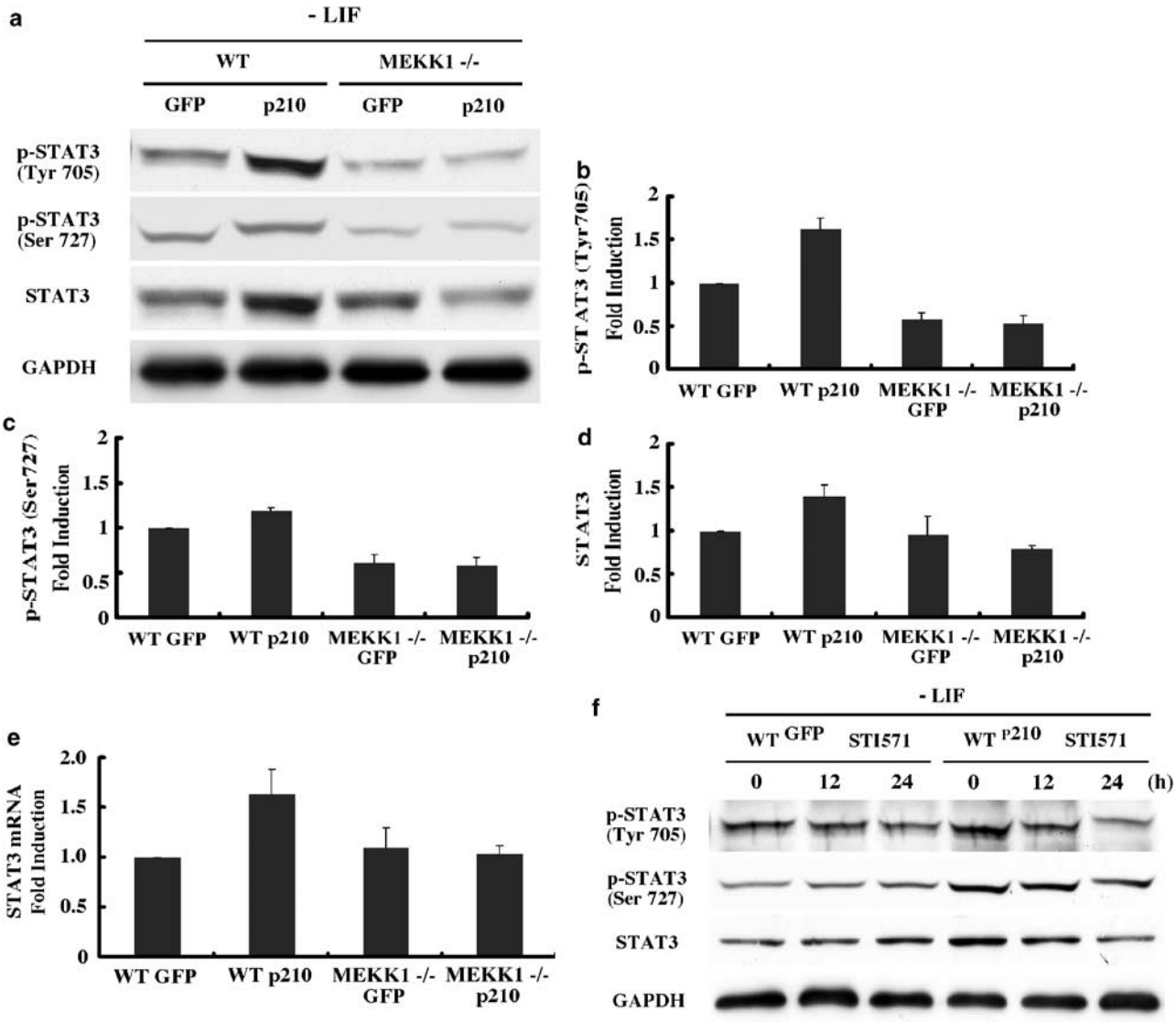

Figure 3 MEKK1 is required for Bcr–Abl-induced STAT3 expression and phosphorylation. (**a**) ES cells were seeded onto uncoated culture dishes in the absence of LIF. After incubating for 2 days, the cells were harvested and lysed, and the lysates were immunoblotted for STAT3 and phospho-STAT3 (Tyr705 and Ser727). The intensities of the specific bands ((**b**) phospho-STAT3 (Tyr705), (**c**) phospho-STAT3 (Ser727), (**d**) STAT3) were determined using NIH Image software. The values of WT^{GFP} were defined as 1.0 for each experiment. Data represent means$\pm$s.d. of three independent experiments. (**e**) In the absence of LIF, total RNA was extracted, reverse-transcribed to cDNA and amplified by PCR. The relative level of STAT3 mRNA is expressed as the ratio of the levels of STAT3 and β-actin mRNAs. The values of WT^{GFP} were defined as 1.0 for each experiment. Data represent means$\pm$s.d. of three independent experiments. (**f**) In the absence of LIF, GFP- or Bcr–Abl-transformed WT ES cells were treated with 10 μM STI571 for the indicated times, after which the cell lysates were immunoblotted for STAT3 and phospho-STAT3 (Tyr705 and Ser727). Levels of GAPDH confirmed that equivalent amounts of protein had been loaded into each lane. The immunoblotting shown is representative of three independent experiments yielding similar results (**a**, **f**)

expression of STAT3 mRNA to be correlated with expression of the protein in the absence of LIF (Figure 3e). Thus, Bcr–Abl appears to enhance STAT3 expression via MEKK1 at the transcriptional level. Moreover, STI571 elicited a time-dependent decline in the expression and phosphorylation of STAT3 in WT^{p210} cells, but not in WT^{GFP} cells (Figure 3f), suggesting that Bcr–Abl tyrosine kinase activity contributes to both the expression and phosphorylation of STAT3 in the absence of LIF.

We used electrophoretic mobility shift assays (EMSAs) to evaluate the binding of STAT3 to DNA in the nucleus. In the absence of LIF, higher levels of STAT3 binding to DNA were detected in WT^{p210} than WT^{GFP} cells, though no difference was detected between MEKK1$-/-^{GFP}$ and MEKK1$-/-^{p210}$ cells (Figure 4a). That STAT3 was bound to its physiological binding site is suggested by our finding that formation of the STAT3–DNA complex was competitively inhibited in the presence of an excess of unlabeled SIEm67 (data not shown). Additional evidence that Bcr–Abl induces nuclear translocation of both total and phosphorylated STAT3 via MEKK1 was obtained when nuclear and cytoplasmic lysates were immunoblotted with anti-STAT3 and anti-phospho-STAT3 (Tyr705). The results showed that nuclear levels of phospho-STAT3 paralleled those of total STAT3 (Figure 4b) and were correlated with STAT3–DNA-binding activity. The physiological nature of the STAT3 binding was further substantiated by luciferase assays, which showed that the transcriptional activity of STAT3 in the absence of LIF was consistent with the results of both the immunoblot analyses and EMSAs (Figure 4c). Furthermore, reconstitution of MEKK1−/− ES cells by transfecting them with WT MEKK1 (MEKK1 add-back) restored the ability of Bcr–Abl to activate STAT3 (Figure 4d), confirming that MEKK1 is required for Bcr–Abl-induced STAT3 activation.

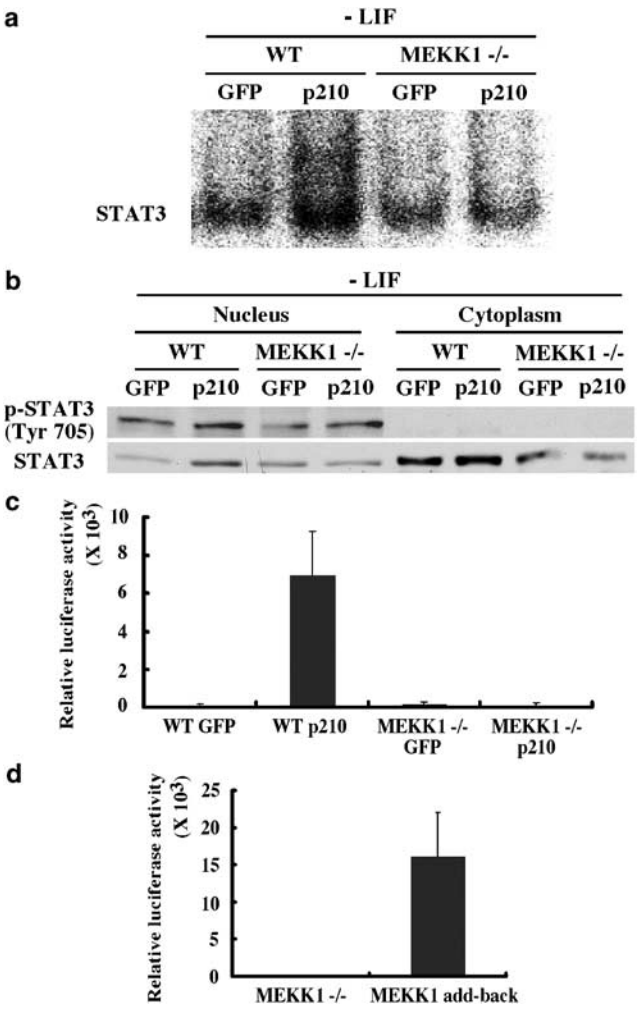

Figure 4 MEKK1 is required for Bcr–Abl-induced STAT3 transcriptional activation. (**a**) Samples (20 μg) of nuclear extract were subjected to EMSA, using SIEm67 as a probe in the absence of LIF. The autoradiogram shown is representative of three independent experiments yielding similar results. (**b**) In the absence of LIF, 25 μg of lysate from the nuclear and cytoplasmic fractions was subjected to immunoblot analysis with anti-STAT3 and anti-phospho-STAT3 (Tyr705). (**c**) In the absence of LIF, ES cells were transiently transfected with 3 μg of pTA-Luc or pSTAT3-TA-Luc, together with 2 μg of β-galactosidase reporter vector. At 24 h after transfection, cell lysates were prepared and assayed for luciferase activity. (**d**) In the absence of LIF, MEKK1−/− and MEKK1-add-back ES cells were transiently transfected with 2 μg of pTA-Luc or pSTAT3-TA-Luc, together with 2 μg of p210 Bcr–Abl expression vector and 1 μg of β-galactosidase reporter vector. At 24 h after transfection, cell lysates were prepared and assayed for luciferase activity. Luciferase assays were normalized to the corresponding β-galactosidase activity. Data represent means$\pm$s.d. of three independent experiments (**c**, **d**)

Bcr–Abl-induced MEKK1–STAT3 pathway is not involved with ERK, JNK, JAK2 or Rac1

Bearing in mind that MEKK1 is a physiological regulator of JNK and ERK (Yujiri *et al*., 1998), we next investigated which intracellular signaling protein(s) is involved in the Bcr–Abl–MEKK1–STAT3 pathway. Immunoblot analyses using phosphospecific Abs showed that Bcr–Abl enhanced ERK activation in both WT^{p210} and MEKK1$-/-^{p210}$ cells in the absence of LIF. On the other hand, JNK activation was not elevated in either cell type (Figure 5a), and MEKK1$-/-^{GFP}$ and MEKK1$-/-^{p210}$ cells, respectively, showed less ERK activity than WT^{GFP} and WT^{p210} cells (Figure 5a).

Treating WT^{p210} cells with the MEK1/2 inhibitor U0126 completely blocked ERK activity, reducing phosphorylation of STAT3 on Ser727 but not on Tyr705; STAT3 binding to DNA was unaffected (Figure 5b). Although ERK activity has been linked to STAT3 Ser727 phosphorylation and to the negative regulation of STAT3 activity (Decker and Kovarik, 2000), our result indicates that Bcr–Abl-induced ERK activation does not contribute to the STAT3 activation seen in the absence of LIF. In addition, the reduced ERK activity seen in MEKK1$-/-^{p210}$ cells did not cause a decrease in STAT3 activation.

Janus kinase 2 (JAK2) is also a physiological regulator of STAT3 activation (Hirano *et al*., 2000), but we found that tyrosine phosphorylation of JAK2 –

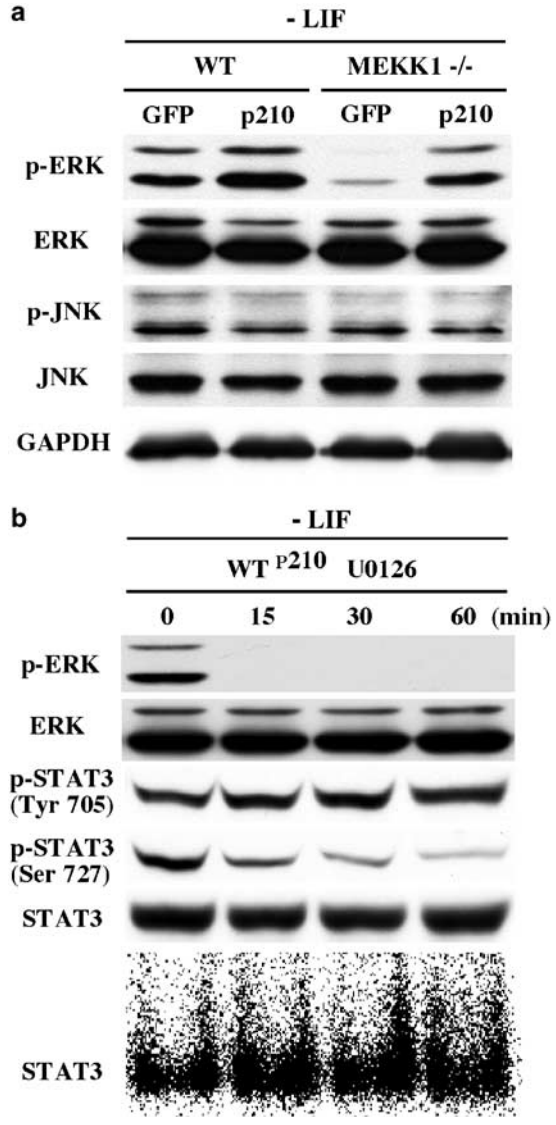

Figure 5 Bcr–Abl-induced STAT3 activation is not via ERK or JNK. (**a**) In the absence of LIF, ES cell lysates were immunoblotted for ERK2, phospho-ERK, JNK1 and phospho-JNK. Levels of GAPDH confirmed that equivalent amounts of protein had been loaded into each lane. (**b**) In the absence of LIF, Bcr–Abl-transformed WT ES cells were treated with 10 μM U0126 for the indicated times, after which whole-cell lysates were immunoblotted for STAT3 and phospho-STAT3 (Tyr705 and Ser727), and nuclear extracts were subjected to EMSA using SIEm67 as a probe. The data shown are representative of three independent experiments yielding similar results

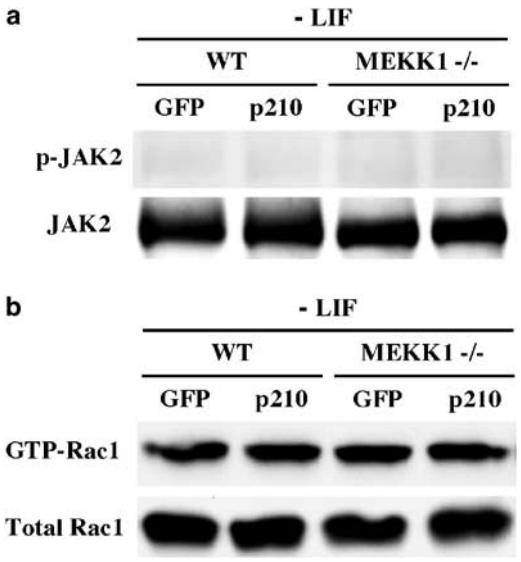

Figure 6 Bcr–Abl-induced STAT3 activation is not via JAK2 or Rac1. (**a**) In the absence of LIF, ES cell lysates were immunoprecipitated for JAK2 and immunoblotted with 4G10 and anti-JAK2 Ab. (**b**) In the absence of LIF, ES cell lysates were harvested, and the amount of GTP-bound Rac1 (GTP-Rac1) was determined using PAK1 pull-down assays. In addition, a portion (1/10) of the cell lysate was subjected to immunoblot analysis to determine the total amount of Rac1 in each sample. The immunoblotting shown is representative of three independent experiments yielding similar results

and thus its activation – was unaffected by Bcr–Abl (Figure 6a).

Finally, we assessed the activity of the small GTPase Rac1 because it reportedly regulates epidermal growth factor (EGF)-mediated STAT3 activation (Simon *et al*., 2000) and is activated by Bcr–Abl (Skorski *et al*., 1998), and because MEKK1 reportedly associates with GTP-bound active Rac1 (Fanger *et al*., 1997). We found that levels of GTP-bound Rac1 were not increased by Bcr–Abl in ES cells (Figure 6b). Collectively, therefore, our findings suggest that Bcr–Abl activates an MEKK1–STAT3 pathway, though not through ERK, JNK, JAK2 or Rac1.

Discussion

During the chronic phase of CML, Bcr–Abl-expressing leukemic stem cells are characterized by their persistent ability to differentiate towards all hematopoietic lineages. The signaling pathway by which the Bcr–Abl-expressing clone expands and undergoes self-renewal remains largely unknown, however. We therefore used murine undifferentiated ES cells to investigate the early molecular events that occur in Bcr–Abl-associated leukemogenesis. As reported previously (Coppo *et al*., 2003), Bcr–Abl-expressing ES cells persistently exhibited a primitive morphology, despite LIF withdrawal. In addition, like Bcr–Abl-transformed 32D and Ba/F3 cells (Nawata *et al*., 2003), they showed enhanced MEKK1 expression and activation.

To define the significance of MEKK1 activation in Bcr–Abl-induced leukemogenesis, we compared Bcr–Abl-induced transformation of WT and MEKK1-deficient ES cells. Surprisingly, the ability of Bcr–Abl, in the absence of LIF, to induce changes in both the morphology of ES cell colonies and alkaline phosphatase activity that were consistent with an undifferentiated phenotype was MEKK1-dependent, suggesting that MEKK1 plays a key role in Bcr–Abl-induced

self-renewal of ES cells via a Bcr–Abl-mediated transformation pathway.

The role of STAT3 activation in the promotion of self-renewal in ES cells is well established; indeed, constitutive activation of STAT3 has been shown not only in Bcr–Abl-expressing ES cells but also in primary CML cells (Coppo *et al*., 2003). Nevertheless, it was unexpected that MEKK1 would be required for Bcr–Abl-induced STAT3 activation in ES cells. Our findings with genetically deficient cells enable us to report for the first time that not only is MEKK1 involved in STAT3 activation but also its action is independent of MAPK family pathways. By transfecting cells with MEKK1 cDNA, Lim and Cao (2001) showed that MEKK1 regulates growth factor-induced STAT3 activation and phosphorylation of STAT3 protein on both Tyr705 and Ser727. We found that Bcr–Abl induces constitutive activation of ERK, but not JNK, JAK2 or Rac1, which have been thought to regulate STAT3 activation. In addition, treating cells with an MEK inhibitor showed that the MEKK1–ERK pathway does not contribute to Bcr–Abl-induced STAT3 activation. It is thus plausible that MEKK1 directly regulates the activation of STAT3 in Bcr–Abl-expressing stem cells.

In conclusion, our findings suggest that MEKK1 plays a key role in self-renewal and STAT3 activation in Bcr–Abl-transformed ES cells. Although it remains to be determined precisely how MEKK1 contributes to Bcr–Abl-induced transformation of hematopoietic stem cells, our findings suggest that MEKK1 may be a useful therapeutic target for the treatment of CML.

Materials and methods

Cell culture

WT, MEKK1−/− and MEKK1 add-back CCE ES cells (Yujiri *et al*., 1998) were maintained on gelatin-coated dishes in DMEM (Invitrogen) supplemented with 25 mM Hepes, 100 U/ml penicillin, 100 mg/ml streptomycin (Invitrogen), 15% fetal bovine serum (Equitech-Bio, Inc.), 0.5% LIF-conditioned medium and 0.14 mM monothioglycerol (Sigma). Bcr–Abl-expressing ES cells were selected by adding 0.8 μg/ml puromycin to the ES cell culture medium. All of these cell lines were used as monoclonal cell mixtures.

Materials

Anti-c-Abl Ab was purchased from Oncogene Research. Anti-MEKK1, -ERK2, -JNK1 and -phospho-JNK Abs were from Santa Cruz Biotechnology. Anti-STAT3, -phospho-STAT3 (Tyr705), -phospho-STAT3 (Ser727) and -phospho-ERK Abs were from Cell Signaling Technology. Anti-JAK2 and -Rac1 Abs were from Upstate Biotechnology. Antiglyceraldehyde-3-phosphate dehydrogenase (GAPDH) Ab was from Chemicon. 4G10 antiphosphotyrosine mAb is described elsewhere (Ogihara *et al*., 1997). U0126 was from Calbiochem. STI571 was kindly provided by Novartis (Basel, Switzerland). Stock solutions of U0126 (10 mM) and STI571 (10 mM) were prepared in dimethylsulfoxide and stored at −80 and −20°C, respectively. Appropriate drug concentrations were made by dilution with fresh medium immediately before each experiment. The retroviral vector pMY was prepared as described previously (Nawata *et al*., 2003). p210 Bcr–Abl cDNA was a gift from Dr Owen N Witte (UCLA). WT and MEKK1−/− ES cells were stably transformed with pMY-GFP or pMY-p210-Bcr–Abl. pGEX-2T-PAK was kindly provided by Dr Yoh Takuwa (Kanazawa University).

Immunoblotting and immunoprecipitation

ES cells were lysed as described previously (Nawata *et al*., 2003). For immunoprecipitation, the lysates were incubated first with anti-c-Abl or anti-JAK2 Ab for 2 h at 4°C and then with protein G-Sepharose (Amersham Biosciences) for an additional 3 h. The Sepharose beads were then washed two times in lysis buffer and resuspended in Laemmli sample buffer. The immunoprecipitates were resolved by SDS–PAGE.

Alkaline phosphatase staining

ES cell colonies were fixed and stained for alkaline phosphatase using naphthol/fast red violet solution following the manufacturer's instructions (Chemicon). Numbers of alkaline phosphatase-positive colonies were scored by microscopic examination.

Semiquantitative RT–PCR

Total RNA was extracted from ES cells using ISOGEN (Nippongene, Toyama, Japan) according to the manufacturer's protocol, after which cDNA was synthesized using SuperScript II (Invitrogen) with 1-μg aliquots of total RNA. PCR was then run for 25 cycles, and primer annealing for STAT3 was carried out at 58°C for 1 min. The sequences of the PCR primers were: for STAT3, 5′-ATG AAG AGT GCC TTC GTG GTG G-3′(sense) and 5′-GGA TTG ATG CCC AAG CAT TTG G-3′ (antisense), and for β-actin, 5′-ATG TGC AAG GCC GGC TTC GCG GGC GAC G-3′ (sense) and 5′-CAG CCA GGT CCA GAC GCA GGA TGG CAT-3′ (antisense). Thereafter, 10 μl of each PCR product was electrophoresed on 2.0% agarose gels, and the intensities of the specific bands were determined using NIH Image software. As an internal control, the relative level of STAT3 mRNA was normalized to that of β-actin mRNA.

Electrophoretic mobility shift assay (EMSA)

Nuclear protein extracts were prepared from ES cells as described previously (Nawata *et al*., 2003), after which aliquots of the extract were preincubated for 15 min at room temperature with 0.8 μg of poly(dI-dC) in binding buffer (20 mM Tris-HCl (pH 7.5), 50 mM potassium chloride, 5% glycerol, 1 mM dithiothreitol, 1 mM EDTA and 0.1% NP40). A ^{32}P-labeled DNA probe for the STAT3-binding site SIEm67 (Sadowski *et al*., 1993) was then added, and the incubation was continued for an additional 15 min. Finally, the DNA–protein complexes were separated on a 6% polyacrylamide gel and exposed for autoradiography.

Luciferase assays

Using FuGENE6 (Roche), ES cells were transiently transfected with 3 μg of pTA-Luc or pSTAT3-TA-Luc vector (Clontech), together with 2 μg of the β-galactosidase reporter vector CH110 (Promega). The negative control (pTA-Luc) lacks the STAT3 enhancer element, but contains a TATA box promoter and luciferase reporter gene. pSTAT3-TA-Luc contains four copies of the STAT3 enhancer element (TGCTTCCCGAACGT). At 24 h after transfection, the cells were lysed with PicaGene reporter lysis buffer (Toyo Inki,

Tokyo, Japan), and the luciferase activity in the lysates was measured using a PicaGene luciferase assay kit (Toyo Inki, Tokyo, Japan). To control for variation in transfection efficiency, luciferase activity was normalized to the corresponding β-galactosidase activity. The values obtained from controls (pTA-Luc) were subtracted from experimental results (pSTAT3-TA-Luc).

Measuring GTP-Rac1 levels

Levels of activated, GTP-bound Rac1 were measured using PAK1 pull-down assays as described previously (Okamoto *et al*., 2000). Briefly, the cells were collected and lysed, after which the lysates were clarified and incubated with GST-PAK1 (amino acids 75–131) on beads to capture GTP-bound Rac1 proteins. The bound proteins were washed three times and eluted with sample buffer before being subjected to SDS–PAGE and immunoblotted with an anti-Rac1 Ab. Whole-cell lysates (10% of input) were analysed in parallel.

Acknowledgements
We thank Drs Owen N Witte and Yoh Takuwa for the generous gift of plasmids. We also thank Drs Takumi Era (RIKEN), Keisuke Hagihara, and Kazuyuki Yoshizaki (Osaka University) for valuable discussions; Yukari Kora and Atsuko Tanimura for technical assistance. This work was supported by a grant-in-aid from the Ministry of Education, Culture, Science and Sports of Japan (to TY).

References

Burdon T, Smith A and Savatier P. (2002). *Trends Cell Biol.*, **12,** 432–438.
Coppo P, Dusanter-Fourt I, Millot G, Nogueira MM, Dugray A, Bonnet ML, Mitjavila-Garcia MT, Le Pesteur D, Guilhot F, Vainchenker W, Sainteny F and Turhan AG. (2003). *Oncogene*, **22,** 4102–4110.
Decker T and Kovarik P. (2000). *Oncogene*, **19,** 2628–2637.
Deininger MW, Goldman JM and Melo JV. (2000). *Blood*, **96,** 3343–3356.
Druker BJ. (2002). *Oncogene*, **21,** 8541–8546.
Fanger GR, Johnson NL and Johnson GL. (1997). *EMBO J.*, **16,** 4961–4972.
Hagemann C and Blank JL. (2001). *Cell Signal.*, **13,** 863–875.
Hirano T, Ishihara K and Hibi M. (2000). *Oncogene*, **19,** 2548–2556.
Holyoake T, Jiang X, Eaves C and Eaves A. (1999). *Blood*, **94,** 2056–2064.
Lim CP and Cao X. (2001). *J. Biol. Chem.*, **276,** 21004–21011.
Nawata R, Yujiri T, Nakamura Y, Ariyoshi K, Takahashi T, Sato Y, Oka Y and Tanizawa Y. (2003). *Oncogene*, **22,** 7774–7780.
Ogihara T, Shin BC, Anai M, Katagiri H, Inukai K, Funaki M, Fukushima Y, Ishihara H, Takata K, Kikuchi M, Yazaki Y, Oka Y and Asano T. (1997). *J. Biol. Chem.*, **272,** 12868–12873.
Okamoto H, Takuwa N, Yokomizo T, Sugimoto N, Sakurada S, Shigematsu H and Takuwa Y. (2000). *Mol. Cell. Biol.*, **20,** 9247–9261.
Pease S, Braghetta P, Gearing D, Grail D and Williams RL. (1990). *Dev. Biol.*, **141,** 344–352.
Sadowski HB, Shuai K, Darnell Jr JE and Gilman MZ. (1993). *Science*, **261,** 1739–1744.
Simon AR, Vikis HG, Stewart S, Fanburg BL, Cochran BH and Guan KL. (2000). *Science*, **290,** 144–147.
Skorski T, Wlodarski P, Daheron L, Salomoni P, Nieborowska-Skorska M, Majewski M, Wasik M and Calabretta B. (1998). *Proc. Natl. Acad. Sci. USA*, **95,** 11858–11862.
Yujiri T, Sather S, Fanger GR and Johnson GL. (1998). *Science*, **282,** 1911–1914.